Journal of Solid Mechanics Vol. 12, No. 3 (2020) pp. 620-631
DOI: 10.22034/jsm.2019.1882104.1511

Numerical Analysis of the Effect of External Circumferential Cracks in Transition Thickness Zone of Pressurized Pipes Using XFEM – Elastic-Plastic Behavior

H. Salmi [1, *], Kh. EL Had [2], H. EL Bhilat [1], A. Hachim [2]

[1] *Department of National Higher School of Mechanics, ENSEM, Laboratory of Control and Mechanical Characterization of Materials and Structures, Morocco*
[2] *Institute of Maritims Studies, Laboratory of Materials and Structures Casablanca, Morocco*

Received 22 June 2020; accepted 20 August 2020

ABSTRACT

The elastic-plastic behavior of the material is considered to analyze the effect of an external circumferential crack on a pipe with thickness transition and double slopes. Using the extended finite element method (XFEM), the *J*-integral of 3D cracks were investigated and compared between straight pipes and pipes with thickness transition and different slopes. Considering internal pressure, this work highlighted the investigation of a 3D crack problem in a thickness transition pipe with a double slope, In the extended finite element method (XFEM), the level sets and the enrichment zone were defined. A crack is easily modeled by enrichment functions. The comparison between the values of the *J*-integral showed that the pipe containing thickness transition with double slopes is more sensitive to the considered cracks, more precisely, the parameters of the first thickness transition have more influence on the variation of *J*-integral than the parameters of the second thickness transition. The decreasing of the angle of the slopes and the increase of the ratio of the thicknesses is one effective method of reducing the *J*-integral.

Keywords: Elastic-plastic; Pipe with thickness transition and double slope; Three-dimensional crack; XFEM; *J*-integral.

1 INTRODUCTION

PRESSURE equipment is found in industrial plants, especially those related to energy production or chemical industry [1-4]. Seeing that the pressure equipment components are mostly made of ductile materials, the elastic-plastic fracture mechanics principles are used to deal with the plasticity ahead of the crack tip, for this goal, the estimation of *J*-integral value is very essential and elastic-plastic finite element analysis is the most general technique to achieve the purpose [5]. The French Alternative Energies and Atomic Energy Commission (CEA) [6] developed a finite element software Castem [7] for structural and fluid mechanics [8-9]. CEA [8-9] used Finite

[*] Corresponding author. Tel.: +66 7209466.
E-mail address: houda.salmi111@gmail.com (H. Salmi).

element method (FEM) to study straight pipes with circumferential cracks by evaluating the stress intensity factor for elastic range and the *J*-integral in elastic-plastic range, Sridhar et al. [10] considered the plastic behavior of the material to study girth welded pipelines with 3D cracks exposed to biaxial loadings; Xiao et al. [11] investigated the fatigue crack growth of offshore pipelines affected by 3D cracks. The field of pressure equipment also concerns pipe with thickness transition, these structures correspond to a connection between pipes with different diameters and they are classified into two types: transitions with a single slope and transitions with a double slope [3,4,12,13]. Piping size change generates a significant stress concentration who should have particular attention in the design of piping; But, in contrast to straight pipes and elbows, much less effort on numeric methods has been made for pipe with thickness transition [14]. In this concept we can cite the works of Saffih [4], based on a numerical study by the FEM; [4] showed that the thickness transition presents the risk zone of the pipe with a single slope. The heavy cost of direct FE calculations [8], motivates the use of other numerical methods such as the mesh free method, the boundary element method and the extended finite element method (XFEM) [15, 16, 17]. Among those methods, XFEM offers great advantages over others, since it enables the mesh to be independent of the evolving crack geometry; In addition, XFEM gives an accurate result, thanks to enrichment functions even with coarse meshes near the crack tip [18]. The XFEM was initiated by Belytschko et Black [19]. Stolarska et al [20] coupled between the level set method (LSM) and XFEM to investigate the problem of cracks. XFEM has some limitations such as the description of the plastic behavior of the material at the crack tip, in order to overcome that, Sachin Kumar [21] proposed an elastic-plastic enrichment basis to represent the singularities in elastic-plastic fracture mechanics. In the field of pressurized equipment, [22] used the XFEM to study the fracture behavior of pipes under internal detonation loads; K. Sharma [23] performed a numerical investigation with XFEM to evaluate the stress intensity factor of a semi-elliptical crack in a pipe band. Using the XFEM to investigate the effect of the crack on a thickness transition and evaluating the influence of transition zone on J-integral was however not treated in [3,4,12,13], also, taking account of the second slope of thickness transition was required to complete the work in [3,4,12,13].

The purpose of this work is the application of XFEM to evaluate the effect of a 3D circumferential crack in thickness transition with a double slope in a pipe and investigate the effect of the parameters of the transition zone on *J*-integral in elastic-plastic behavior. In section 2, the theoretical method to calculate the *J*-integral is introduced. In section 3, the definition of enrichment zone and the level set is provided at the same time the geometry of the pressure equipment is defined. In section 4, the influence of the parameters of the transition zone on the *J*-integral is discussed. Finally, a comparative study of the *J*-integral is done between straight pipes and pipes with the thickness transition with different slopes.

2 MATHEMATICAL FORMULATION

2.1 J- integral for a circumferential crack in a straight pipe

For elastic-plastic behavior of a material with hardening effect, the *J*-integral can be expressed by Eq. (1) [24-26]:

$$J = J_e\left(a_e\right) + J_p \tag{1}$$

where J_e and J_p are respectively the elastic and plastic part of J:

$$J_e = \frac{K^2}{E'} \quad \text{with } E' = \frac{E}{(1-\vartheta^2)} \quad \text{in plane strain} \tag{2}$$

The stress intensity factor is given by Eq. (3).

$$K = \sigma i_0 \sqrt{\pi a_e} \tag{3}$$

where i_0 is the elastic influence function for *J*-integral. In general, it is enough to judge the severity of the defect by evaluating *K* (*J* for elastic-plastic range) only by a weighted-average of local *K*-values (*J*-values) calculated at inside J_1, middle J_2, and outside J_3 crack-tips, the average value of *K* or *J* is given by Eqs. (4) and (5)[8].

$$K = \frac{1}{6}(K_1 + 4K_2 + K_3) \text{ for elastic range} \tag{4}$$

$$J = \frac{1}{6}(J_1 + 4J_2 + J_3) \text{ for elastic-plastic range} \tag{5}$$

a_e is the corrected crack depth in order to incorporate the effect of plastic deformation near the crack tip. Irwin [27]:

$$a_e = a + \frac{1}{\pi\beta}\left(\frac{K(a)}{\sigma_0}\right)^2 \tag{6}$$

with a is the crack depth, $\beta = 2$ for plane stress, and $\beta = 6$ for plane strain conditions.

In general, the pipe can be exposed to different types of loads (Fig.1(a)), axial loading, bending moment or internal pressure [8-10], each loading condition or the combination of these types of loads generate the applied stress σ inside the pressurized pipe. [8]

The value of internal pressure is calculated according to the CODAP (C2.1.4.2) instructions [28]:

$$P = \frac{2 \times \sigma \times t \times z}{D_m} \tag{7}$$

where $D_m = 2.R_m = R_i + R_e$ is the mean radius of the pipe with circumferential crack, z is the welding coefficient, for an exceptional situation of service or resistance test, $z = 1$. t is the minimum thickness required of the cylindrical shell. σ is the applied stress in a pipe, σ equal to the nominal stress f for purely elastic behavior of the material. For the elastic-plastic range $\sigma = \sigma_e \gg f$, with σ_e is the yield stress(Table.1).

R_i and R_e are respectively inner and outer radius of thin pipe where $R_e = t + R_i$. So, Eq. (7) becomes:

$$P(\frac{R_i}{t}) = \frac{2\sigma}{2(\frac{R_i}{t}) + 1} \quad \text{with} \quad \frac{R_i}{t} = 25 \tag{8}$$

The fully plastic part of the *J*-integral for a circumferential surface crack in pipes, considering internal pressure, can be rewritten as:

$$J_p = \alpha b \sigma_0 \varepsilon_0 h \times \left(\frac{P}{P_0}\right)^{n+1} \tag{9}$$

where $b = (t - a)$ is the uncracked ligament, P is the applied pressure calculated in Eq. (8), P_0 is the plastic limit load for *P*. The limit pressure for perfectly plastic material is given by Eq. (10) [29]:

$$P_0 = \pi\sigma_0\left(R_e^{\,2} - R_i^{\,2}\right)\left[1 - \frac{\theta}{\pi}\frac{a}{t} - \frac{2}{\pi}sin^{-1}\left(\frac{a}{t}\frac{sin\,\theta}{2}\right)\right] \tag{10}$$

with $\theta = c / R_m$ (For the thin-walled pipes with a large diameter), θ is the crack angle and c is the half crack length (Fig.1 (b)), h is the plastic influence functions for *J*-integral, h depends on crack size, pipe geometry, and strain-hardening exponent n. α is a dimensionless constant that depends on n.

In conclusion, in the case of straight pipe with a circumferential surface crack, the analytic formulas of the *J* integral can be written as:

$$J=\frac{\left(\sigma i_0\sqrt{\pi a_e}\right)^2}{E'}+\alpha\left(t-a\right)\sigma_0\varepsilon_0 h\times\left(\frac{\sigma}{\sigma_0\left[1-\frac{\theta}{\pi}\frac{a}{t}-\frac{2}{\pi}\sin^{-1}\left(\frac{a}{t}\frac{\sin\theta}{2}\right)\right]}\right)^{n+1} \tag{11}$$

From Eqs. (9) and (11), we note that the variation of J value depends on the pressure ratio $\left(\frac{P}{P_0}\right)$ or on the stress ratio $\left(\frac{\sigma}{\sigma_0}\right)$, with σ_0 is the yield stress.

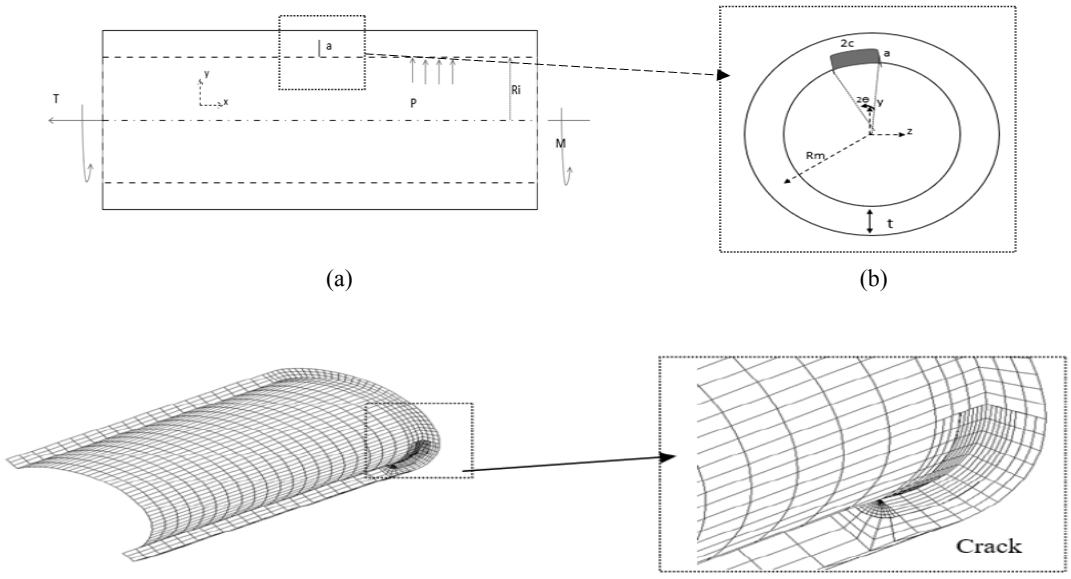

(a) (b)

(c)

Fig.1
Straight pipe with crack: (a) Pressurized pipe exposed to a different load (b) Internal circumferential crack in a pipe (c) The meshing of the cracked pipe.

2.2 J- integral in extended Finite Element Method (XFEM)

The *J*-integral is the energy per unit fracture surface area, in a material [30], in this study, *J* is calculated by the G-Method (Eq. (12)), which is implemented in the software Castem [7]. Sukumar [31] has used the gradient of the level sets to present the crack, [31] has defined this local basis by $e_1=\nabla\psi$, $e_2=\nabla\varphi$ and $e_3=e_1\Lambda e_2$. In XFEM, *J* is expressed on a local basis formed of level set functions [18]:

$$J=\int_{\Gamma_c^+\cup\Gamma_c^-}\theta_i P_{ij} n_j\, d\Gamma-\int_V \theta_i P_{ij}\, dV \tag{12}$$

where P_{ij} is the Eshelby tensor [32], it is given by Eq. (13):

$$P_{ij}=w\,\delta_{ij}-\sigma_{kj}\varepsilon_{ik} \quad (i,j,k)\in\{1,2,3\} \tag{13}$$

with w is the elastic energy density, σ and ε are respectively stress and strain expressed in the basis (e_1,e_2,e_3) (Fig.3). θ is a field of displacement parallel to the plane of the crack and normal to the front (Fig. 2(b)), it is defined by Eq. (14):

$$\theta = \mu e_1 \ , \ \mu(I) = 1 \ \text{ and } \ \mu(x) = 0 \ \text{ for } \ x \in \Gamma_0 \cup \Gamma_1 \cup \Gamma_2 \tag{14}$$

V is a volume containing the crack front C (red arc in Fig. 2(a)) with $V = \Gamma_c^+ \cup \Gamma_c^- \cup \Gamma_0 \cup \Gamma_1 \cup \Gamma_2$. Γ_c^+ and Γ_c^- are the outer and inner surfaces respectively.

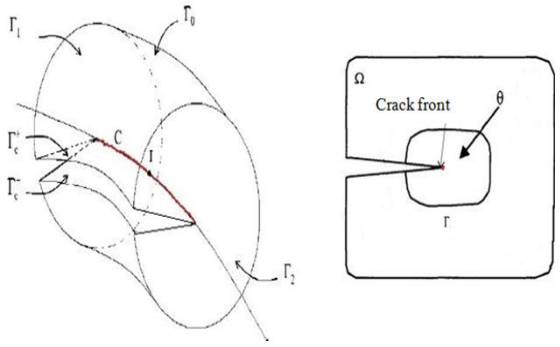

Fig.2
(a) The domain V in integral J computation, (b) example of θ field in 2 dimensions [12].

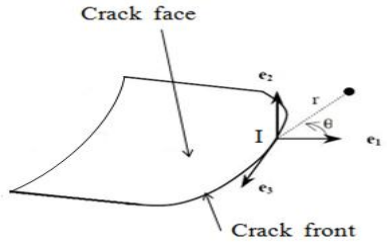

Fig.3
The local basis on the crack front.

3 NUMERICAL SIMULATION

3.1 Geometry and loading

The study considered the material in P265GH steel specially used in pressure equipment, this material is supposed to be elastic-plastic with kinematic hardening $H = 200000 MPa$. Table 1 presents the P265GH steel properties:

Table 1
Properties of P265GH steel.

Young's modulus, E, (GPa)	Yield stress, σ_0, (MPa)	Poisson's ratio, ϑ	Breaking stress, σ_u, (MPa)	Nominal stress, f, (MPa)
200	320	0.3	470	148

The type of pipe is defined by the parameter t/R_i [10]:

t/R_i >0.1: the pipe is thick.

t/R_i <0.1: the pipe is thin.

t/R_i =0.1: the pipe has an average thickness.

In this work, we considered a thin pipe t/R_i =0.04 where t=20 mm. The pipe with thickness transition is subjected to internal pressure, P (Eqs. (7-8)). P/P_0 is varied within the range {0.1; 0.2; 0.4; 0.6; 0.8; 1; 1.2; 1.4}.

The shape of the studied defect is axisymmetric circumrenal external crack (Fig. 4 (b)). It is characterized by the depth 'a'; the total length '2c' and the crack angle 'θ'; in this study $\theta = c/R_m$.

The normalized crack length (θ/π) takes the values 0.01; 0.02; 0.04; 0.06; 0.08. We used the parameter c, to define the crack elongation on the wall of the pipe.

In order to study an extended configuration of the types of defect, we used the parameter (a/t) to define the depth of the crack in the pipe wall, the parameter (a/t) gives several types of defect: shallow crack for (a/t) <0.5 until deep crack for (a/t) = 0.8.

In the present paper, (*a/t*) takes values 0.1, 0.2,0.3, 0.4. This gives a set of 160 configurations of pipe under internal pressure.

This study considered straight pipe (*t*) and pipe with thickness transition (t, t_2, t_3). In industry, pipe with thickness transition is in general used as a concentric or eccentric reducer [33]. Cracks are considered to be located at the base of the transition in the thin part of the pipe [3, 12, 33] (Figs. 4).

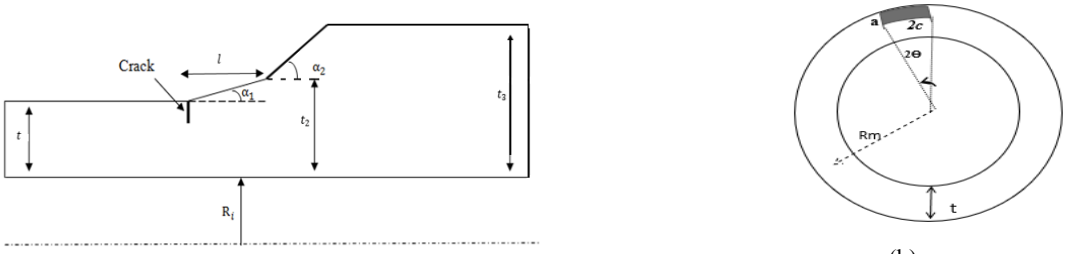

(a) (b)

Fig.4
Cracked pipe with thickness transition: (a) Double slopes thickness transition (b) External circumferential crack in the pipe.

3.2 Crack meshing and enrichment

Applying the symmetry, we model only the half-pipe with thickness transition and an external circumferential crack (Fig. 4(b)), we used 2350 quadrangle elements (XC8R) with 512 Gauss points in block crack, for the rest of the mesh, we used 14950 standard elements (CUB8). The pipes thickness variations are generally located at the outlet of valves (reservoirs), therefore in boundary conditions, we fixed the displacement of the end of the thicker part of the pipe, in addition, we blocked the translation and the rotation in u_y and u_z axes by applying symmetry boundary conditions (Fig. 5(a)). We presented the crack by level sets; therefore, we define a normal level set φ (PHI) from the crack front and tangential level function ψ (PSI) from the crack face (Fig. 5(b)). The sign and the absolute value of the level sets give the distance and the location of the points of solid relative to the crack defined by the set: for a point *x* of the solid (Fig. 6):

$$x \in crack \Rightarrow \{^{\varphi(x)=0}_{\psi(x)\le 0} \quad \text{with } (|\nabla\psi| = |\nabla\varphi| = 1) \tag{15}$$

XFEM analysis by commercial software Castem [7] is conducted; it has the XFEM capabilities for the elastic-plastic behavior of the material with hardening effect. It calculates the *J* integral with the G-Theta method (Eq. (12)).

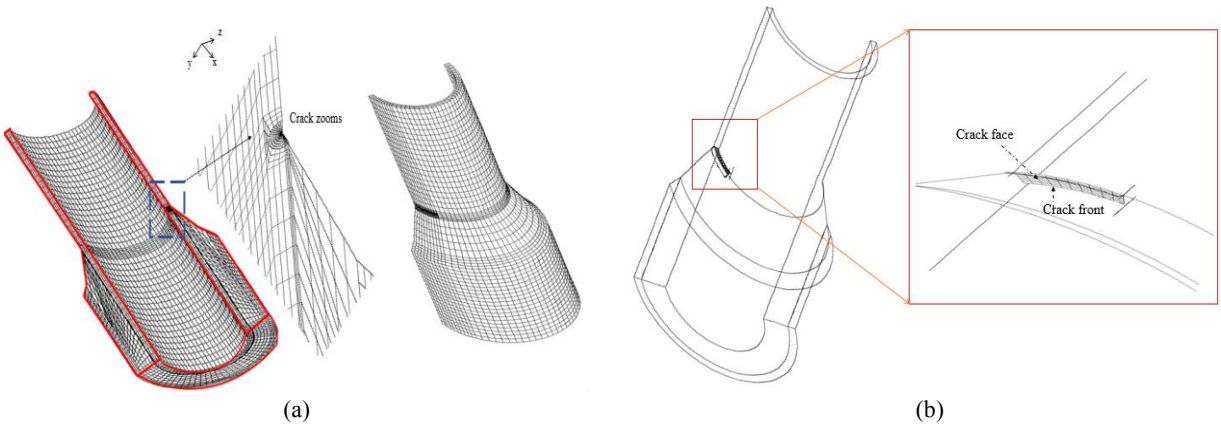

(a) (b)

Fig.5
(a) Cracked half –pipe with double slopes thickness transition, (b) meshing of the crack.

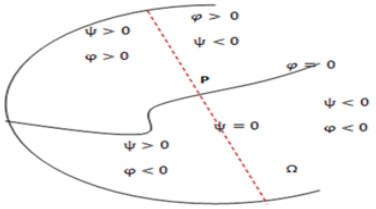

(a)

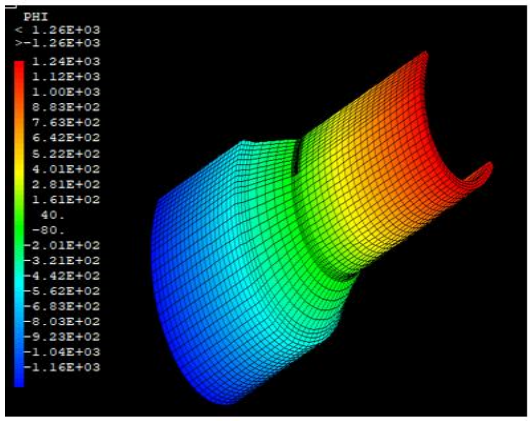

(b)

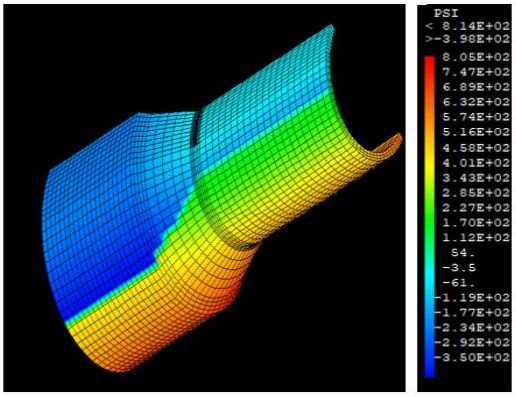

(c)

Fig.6
(a) Representation of a crack with level sets, (b) normal level set, PHI, (c) tangential level set, PSI.

4 RESULTS AND DISCUSSIONS

4.1 XFEM model validation

In order to verify the 3-D elastic-plastic extended finite element model, a straight pipe model is first generated taking account of a small circumferential surface crack (Fig.1) subjected to internal pressure. The pipe has the followed parameters: the thickness of the pipe is *t*=20 *mm*, $t/R_i = 0.04$, the half crack angle θ/π =0.01 and 0.08, Young's modules *E*= 20000 *MPa*, σ_0 =320 *MPa*, α=1 and *n*=15, Poisson's ratio is 0.3. We calculated the mean values of *J*, numerically with XFEM for all values of *a/t*, θ/π and P/P_0. We compared the numerical values of *J* with analytical elastic-plastic solutions of *J* integral in the previous studies (Eq. (11)) [29]. Figs. 7-8 present the evolution of the values of *J*-integral according to the loads and crack depth (*a/t*). The results show a good concordance between the XFEM results and the literature [29], this gives confirmation to use numerical simulation based on XFEM to investigate the *J* integral at a thickness transition of pressurized pipe.

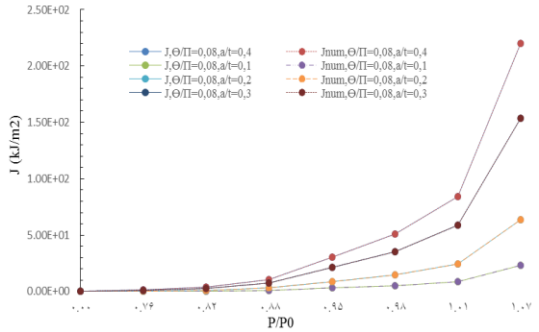

Fig.7
Comparisons of the values of *J* in this study with the analytical solution [29], θ/π =0.08, t/R_i =0.04.

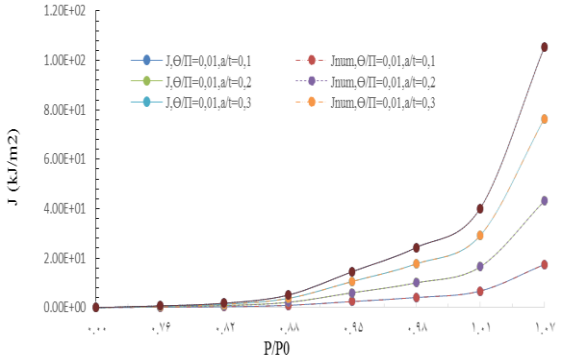

Fig.8
Comparisons of the values of J in this study with the analytical solution [29], θ/π =0.01, t/R_i =0.04.

4.2 Effect of loading and crack size on J-integral

In this section, we analyzed the effect of the load on J-integral. The pipe with thickness transition with a double slope is subjected to internal pressure P. The ratio P/P_0 varies within the range {0.1, 0.2… 1.4}. Figs. 9(a) and 9(b), illustrate the variation of the mean value of the J-integral according to the loading for different values of a/t and θ/π. The results show that the J values depend on the crack depth and loading, for the great value of P/P_0 ($P/P_0 \succ 0.5$), the J values increase when P/P_0 and a/t increase. The maximum of J-values is reached for great a value of θ/π, showing clearly that the longest and deepest crack propagates more easily than shallow and slightly elongated crack. This result is logical and it is due to the fact that the cracked zone becomes more stressed in the thickness transition with a double slope, because of the thickness transition which acts as an amplifier of the stress, so stresses are redistributed in the crack plane giving more stressed points.

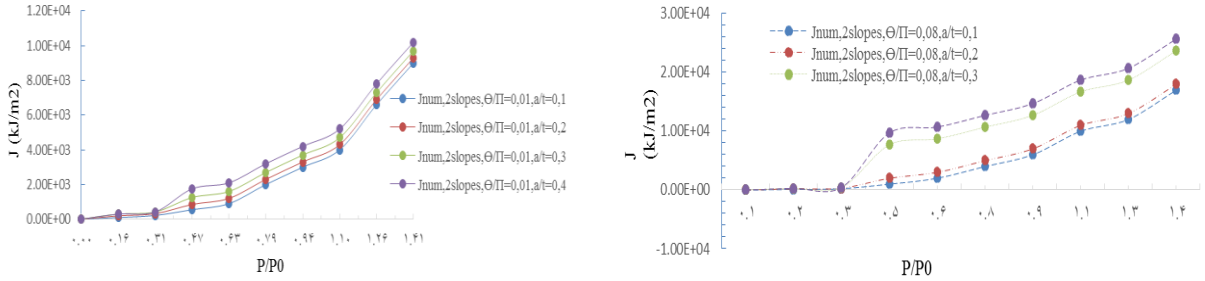

(a) (b)

Fig.9
The variation of J-values according to the loading for different values of a/t , t/R_i =0.04: (a) θ/π =0.01, (b) θ/π =0.08.

4.3 Comparison between J-values of the pipe with uniform thickness and the pipe with thickness transition

Considering the internal pressure, this section compares the values of J-integral of a circumferential crack between different types of pipe: straight pipe, pipe with thickness transition and different slopes. In order to know the harmfulness of a crack in a thickness transition in comparison to the straight pipe, we defined a parameter $S_1 = J_S / J_{T1}$ and $S_2 = J_{T1}/J_{T2}$. Where J_S , J_{T1} and J_{T2} are the value of the J-integral calculated for straight pipe, single-slope thickness transition pipe, and double-slope thickness transition pipe respectively.

Fig. 10 (a-b) illustrate the variations of S_1 according to (P/P_0) for θ/π equal to 0.01 and 0.08 in the case of thin pipes ($t/R_i = 0.04$). Whatever the value of θ/π and a/t ; S_1 is greater than 1, the single-slope thickness transition pipe presents more risk than the straight pipe.

In previous studies [12, 13], we verified that a single-slope thickness transition pipe presents 4 to 6 times risk than uniform thickness pipe for elastic range. However, in this study, for the elastoplastic range, thickness transition tubes are riskier than the straight pipe of an order of a hundred, this mainly for large load value ($P/P_0 \succ 0.8$).Fig. 11 (a-b) present the variation of S_2 according to the loading and crack size. For the small value of loading

($P/P_0 \le 0.5$), single-slope thickness transition pipe and double-slope thickness transition pipe present an almost similar risk. For $P/P_0 \succ 0.5$, the *J*-value of the double-slope thickness transition pipe is 2 to 10 times riskier than the single-slope thickness transition pipe.

The transition reacts as a raiser of stress; it amplified the stress close to the surface. When the applied pressure (*P*) and the depth of the crack (*a/t*) increases, the concentration of the stress increases, so, greater sizes of the defects (deeper or a more elongated cracks)create points with higher stress in the crack plane, and the stresses are more amplified near the surface because of the first and the second thickness transition then $J_{T2} \ge J_{T1} \ggg J_S$.

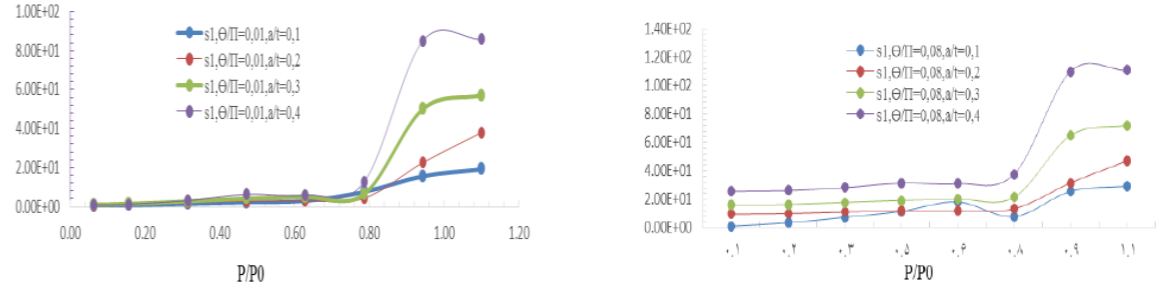

(a) (b)

Fig.10
The variation of S_1 according to (P/P_0), t/R_i =0.04: (a) θ/π =0.01, (b) θ/π =0.08.

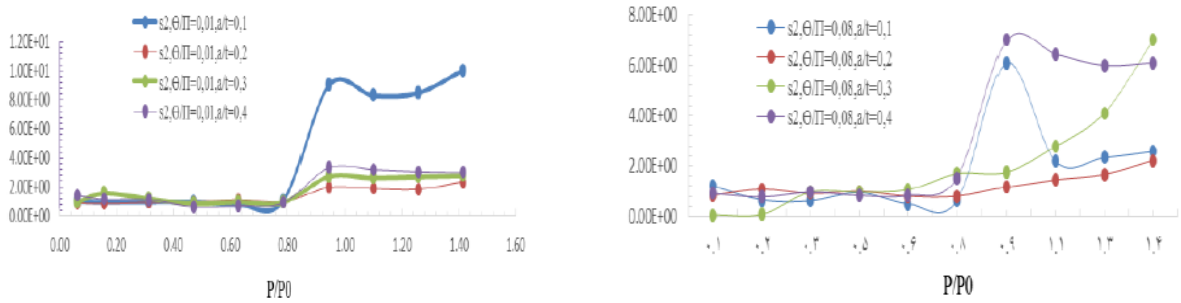

(a) (b)

Fig.11
The variation of S_2 according to (P/P_0), t/R_i =0.04: (a) θ/π =0.01, (b) θ/π =0.08.

4.4 Effect of the transition zone on the variation of J-integral

The thickness transition is related to the angle of the slopes by the following relation:

$$l = t_2\left[\frac{(1-t/t_2)}{\tan(\alpha_1)} + \frac{(t_3/t_2-1)}{\tan(\alpha_2)}\right] \quad \text{with} \quad 0<\alpha_1<\frac{\pi}{2} \quad \text{and} \quad 0<\alpha_2<\frac{\pi}{2} \quad \text{and} \quad t \prec t_2 \prec t_3 \tag{16}$$

(*l*) mainly depends on (t_2/t),(t_3/t_2),(α_1)and (α_2). We consider those parameters as variables and analyze their effect on the variation of *J*-values. The parameters of the geometry of the pipe are varied within the following ranges [34]: $0<\alpha_1 \le 30°$, $0<\alpha_2 \le 45°$, $1.1mm \le t \le 35mm$, $7mm \le t_2 \le 40mm$ *and* $7mm \le t_3 \le 40mm$.

In the previous study [12,3] the most severe case encountered in industrial facilities for a pipe with a single slope thickness transition is a transition with $\alpha_1 = 30^\circ$ and $t_2/t = 1.5$. The decreasing of the angle of slope and the increase of the length of the transition is one effective method of reducing the stress intensity factor for the elastic behavior of the material [12]. Therefore, to know the gravest case of (t_3/t_2) and (α_2), we fixed the parameters of

the first thickness transition and varied the remaining parameters. Fig.12 shows the evolution of *J*-value according to t_3/t_2 and α_2 for $\alpha_1 = 30^\circ$, $t_2/t = 1.5$, $P/P_0 = 1.4$ and $\theta/\pi = 0.08$. The ratio t_3/t_2 is varied from 1.1 to 3.

The results show that for small values of t_3/t_2 ($t_3/t_2 \prec 1.9$), the effect of the angle of the second slope has a very weak effect on *J* variations, but its effect appears noticeably when $t_3/t_2 \geq 2.1$ where *J*-integral reaches the maximum value for $\alpha_2 = 45^\circ$. Therefore, in elastic-plastic range, the second transition with $\alpha_2 = 45^\circ$ and $t_3/t_2 = 2.1$ present the grave case of the double-slope thickness transition pipe. In addition to that, the reducing of the parameter t_3/t_2 lead to decreasing of the *J*-value. We also check the influence of the first thickness transition on the variation of *J*-integral (Fig.13), we consider the parameters of the second thickness transition as constant($\alpha_2 = 45^\circ$ and $t_3/t_2 = 2.1$), we varied (t_2/t)and (α_1).The parameter (α_1) is varied within the range of 5°to 40° and the ratio (t_2/t) is varied from 1.1 to 2.1. We concluded that *J*-values depend on the first slope α_1 for all values of t_2/t . As a result, the parameters of the first thickness transition ((t_2/t), (α_1)) have more influence on the variation of *J*-integral than the parameters of the second thickness transition ((t_3/t_2), (α_2)).

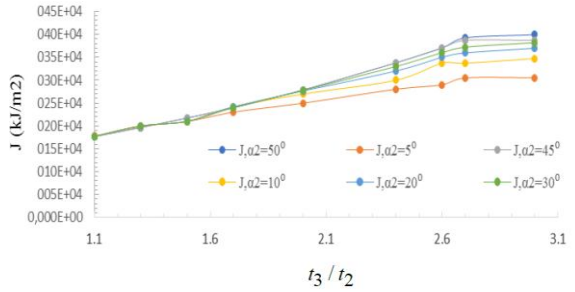

Fig.12
The variation of *J*-values according to t_3/t_2 and α_2, $\alpha_1 = 30^\circ$, $t_2/t = 1.5$, $T/T_0 = 1.4$, $\theta/\pi = 0.08$.

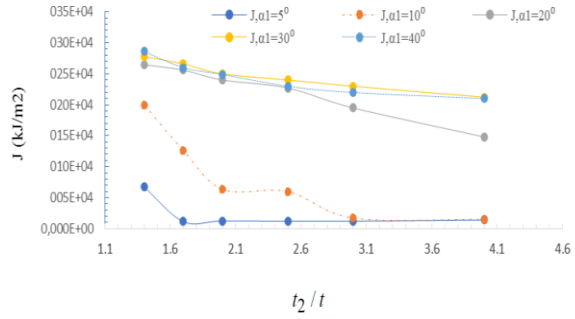

Fig.13
The variation of *J*-values according to t_2/t and α_1, $t_3/t_2 = 2.1$, $\alpha_2 = 45^\circ$, $T/T_0 = 1.4$, $\theta/\pi = 0.08$.

5 CONCLUSION

In this paper, we considered the elastic-plastic behavior of the material; we analyzed the effect of an external circumferential crack located in the thickness transition zone of a pipe with double slopes. The study showed that the angle $\alpha_1 = 30^\circ$ and $1.1 \prec t_2/t \leq 1.5$ are grave cases of the first slope of the thickness transition. The effect of the second slope isn't remarkable, that is to say, the parameters ((t_2/t),(α_1))are more influential than the parameters ((t_3/t_2), (α_2)). Considering the internal pressure, this work highlighted the investigation of a 3D crack problem in a thickness transition pipe with a double slope, using XFEM. In XFEM, the level sets and the enrichment zone were defined. A crack is easily modeled by enrichment functions. The comparison between the values of the *J*-integral showed that the pipe containing thickness transition with double slopes is more sensitive to the considered cracks. The decreasing of the angle of the slopes and the increase of the ratio of the thicknesses of the transition is one effective method of reducing the *J*-integral.

REFERENCES

[1] Rahman S., Ghadiali N., Wilcowski G.M., Moberg F., Brickstad B., 1998, Crack-opening-area analysis for circumferential trough-wall cracks restrain of bending thickness transition and weld residual stresses*, International Journal of Pressure Vessels and Piping* **75**: 397-415.

[2] Électricité de F., 1997, *RSE-M: Règles de Surveillance en Exploitation des Matériels Mécaniques des Ilots Nucléaires REP,* Edition AFCEN.

[3] Abdelkader S., Saıd H., 2006, Numerical study of elliptical cracks in cylinders with a thickness transition, *International Journal of Pressure Vessels and Piping* **83**: 35-41.

[4] Abdelkader S., Saıd H., 2006, Comparison of semi-elliptical cracks in cylinders with a thickness transition and in a straight cylinder – Elastic-plastic behavior, *Engineering Fracture Mechanics* **73**: 2685-2697.

[5] Wessel E.T., Murrysville P.A., Server W.L., Kennedy E.L., 1991, *Primer: Fracture Mechanics in the Nuclear Power Industry***,** EPRI Report, NP-5792-SR**.**

[6] CEA: The French Alternative Energies and Atomic Energy Commission, Commissariat à L'Energie Atomique (France)', http://www.cea.fr/.

[7] CASTEM, http://www-cast3m.cea.fr/

[8] Chapuliot S., Lacire M.H., 1999, Stress intensity factors for external circumferential cracks in tubes over a wide range of radius over thickness ratios, *American Society of Mechanical Engineers*, *Pressure Vessels and Piping Division* **1999** :395-106.

[9] Le Delliou P., Porte P., Code RSE-M: calcul simplifié du paramètre *J* pour un défaut axisymétrique débouchant en surface externe d'une transition d'épaisseur, RAPPORT EDF HT-2C/99/025/A.

[10] Idapalapati S., Xiao Z.M., Yi D., Kumar S.B., 2012, Fracture analysis of girth welded pipelines with 3D embedded cracks subjected to biaxial loading conditions, *Engineering Fracture Mechanics* **96**: 570-587.

[11] Xiao Z., Zhang Y., Luo J., 2018, Fatigue crack growth investigation on offshore pipelines with three-dimensional interacting cracks, *Geoscience Frontiers* **9**(6): 1689-1698.

[12] Salmi H., El Had Kh., El Bhilat H., Hachim A., 2019, Numerical analysis of the effect of external circumferential elliptical cracks in transition thickness zone of pressurized pipes using XFEM, *Journal of Applied and Computational Mechanics* **5**(5): 861-874.

[13] Salmi H**.,** El Had Kh**.,** El Bhilat H**.,** Hachim A**.,** 2019, Numerical modeling and comparison study of elliptical cracks effect on the pipes straight and with thickness transition exposed to internal pressure, using XFEM in elastic behavior, *Journal of Computational and Applied Research in Mechanical Engineering* **5**(5):861-874.

[14] Szu-Ying W., Bor-Jiun T., Jien-Jong Ch., 2015, Elastic-plastic finite element analyses for reducers with constant-depth internal circumferential surface cracks, *International Journal of Pressure Vessels and Piping* **131**: 10-14.

[15] Zhibo M., Zhao Y., 2018,Verification and validation of common derivative terms approximation in meshfree numerical scheme, *Journal of Computational and Applied Research in Mechanical Engineering* **4**(3): 231-244.

[16] Yazdani M., 2018, A novel modification of decouple scaled boundary finite element method in fracture mechanics problems, *JCARME* **7**(2): 243-260.

[17] Surendran M., Pramod A.L.N., Nataraj S., 2019, Evaluation of fracture parameters by coupling the edge-based smoothed finite element method and the scaled boundary finite element method, *Journal of Computational and Applied Research in Mechanical Engineering* **5**(3): 540-551.

[18] Moës N., Gravouil A., Belytschko T., 2002, Non-planar 3D crack growth by the extended finite element and level sets, Part I: Mechanical model, *International Journal for Numerical Methods in Engineering* **53**: 2549-2568.

[19] Belytschko T., Black T., 1999, Elastic crack growth in finite elements with minimal remeshing, *International Journal for Numerical Methods in Engineering* **45**: 601-620.

[20] Stolarska M., Chopp D., Moes N., Belytschko T., 2001, Modelling crack growth by level sets in the extended finite element method, *International Journal for Numerical Methods in Engineering* **51**: 943-960.

[21] Kumar S., Singh I.V., Mishra B.K., 2013, Numerical investigation of stable crack growth in ductile materials using XFEM, *Procedia Engineering* **64**: 652-660.

[22] Malekan M., Khosravi A., Cimini Jr C.A.,2019, Deformation and fracture of cylindrical tubes under detonation loading: A review of numerical and experimental analyses, *International Journal of Pressure Vessels and Piping* **173**: 114-132.

[23] Sharma K., Singh I.V., Mishra B.K., Bhasin V., 2014, Numerical modeling of part-through cracks in pipe and pipe bend using XFEM, *Procedia Materials Science* **6**: 72-79.

[24] Kwang S.W., Prodyot B., 2004, *J*-integral and fatigue life computations in the incremental plasticity analysis of large scale yielding by p-version of F.E.M., *Structural Engineering & Mechanics* **17**(1): 51-68.

[25] Guangzhong L., Guangzhong L., Dai Z., Jin M., Zhaolong H., 2016, Numerical investigation of mixed-mode crack growth in ductile material using elastic-plastic XFEM, *Journal of the Brazilian Society of Mechanical Sciences and Engineering* **38**: 1689-1699.
[26] Liu X., Lu Z.X., Chen Y., Sui Y. L., Dai L.H., 2018, Failure assessment for the high-strength pipelines with constant-depth circumferential surface cracks, *Hindawi Advances in Materials Science and Engineering* **36835**: 1-11.
[27] Irwin G.R., 1961, Plastic zone near a crack and fracture toughness, *Sagamore Research Conference Proceedings* **4**: 63-78.
[28] French construction code, construction des appareils à pression non soumis à l'action de la flamme, The Code for construction of unfired pressure vessels, Division 1, part C – design and calculation, section C2 – rules for calculating cylindrical, spherical and conical shell subjected to internal pressure.
[29] Kumar V., German M., 1988, *Elastic-Plastic Fracture Analysis of Through-Wall and Surface Flaws in Cylinders*, EPRI Topical Report, NP-5596, Electric Power Research Institute, Palo Alto, CA.
[30] Van V., Krystyn J., 2006, *Mechanical Behavior of Materials*.
[31] Sukumar N., Chopp D.L., Moran B., 2003, Extended finite element method and fast marching method for three-dimensional fatigue crack propagation, *Engineering Fracture Mechanics* **70**: 29-48.
[32] Eshelby J.D., 1956, The continuum theory of lattice defects, *Solid State Physics* **3**: 79-144.
[33] Mahaffey R.M., Van Vuuren S.J., 2014, Review of pump suction reducer selection: Eccentric or concentric reducers, *Journal of the South African Instituti Engineering* **56**(3): 65-76.
[34] EL-Gharib J., 2009, Macro commande MACR_ASCOUF_MAIL, Code Aster Clé: U4.CF.10, Révision: 1122, Document diffusé sous licence Gnufdl.